



UNIVERSITI PUTRA MALAYSIA

***MICROSTRUCTURE AND DIELECTRIC PROPERTIES OF YTTRIUM
IRON GARNET-STRONTIUM TITANATE BI-PLATES JUNCTIONS AND
COMPOSITES JUNCTIONS***

WONG SWEE YIN

FS 2017 96



**MICROSTRUCTURE AND DIELECTRIC PROPERTIES OF YTTRIUM IRON
GARNET-STRONTIUM TITANATE BI-PLATES JUNCTIONS AND
COMPOSITES JUNCTIONS**

By

WONG SWEE YIN

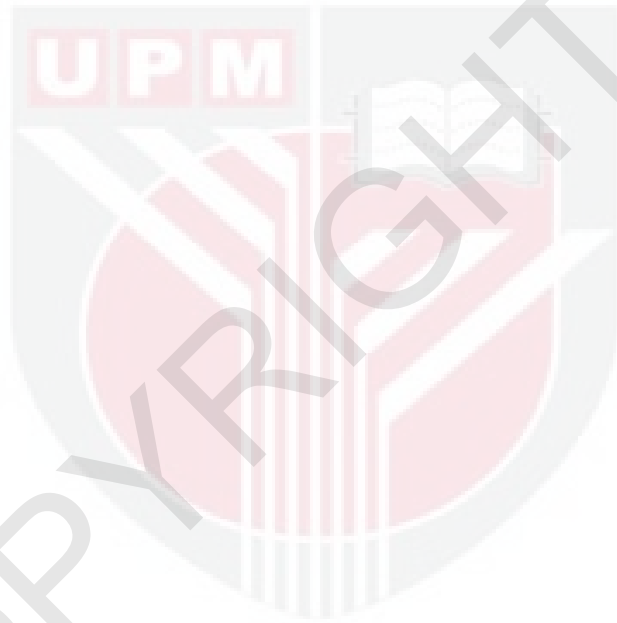
**Thesis Submitted to the School of Graduate Studies, Universiti Putra Malaysia, in
Fulfilment of the Requirement of the Degree of Doctor of Philosophy**

January 2017

COPYRIGHT

All material contained within the thesis, including without limitation text, logos, icons, photographs, and all other artwork, is copyright material of Universiti Putra Malaysia unless otherwise stated. Use may be made of any material contained within the thesis for non-commercial purposes from the copyright holder. Commercial use of material may only be made with the express, prior, written permission of Universiti Putra Malaysia.

Copyright© Universiti Putra Malaysia



Abstract of the thesis was presented to the Senate of Universiti Putra Malaysia
in fulfillment of requirements for the degree of Doctor of Philosophy

**MICROSTRUCTURE AND DIELECTRIC PROPERTIES OF YTTRIUM
IRON GARNET-STRONTIUM TITANATE BI-PLATES JUNCTIONS
AND COMPOSITES JUNCTIONS**

By

WONG SWEE YIN

January 2017

Supervisor : Jumiah Hassan, PhD
Faculty : Science

In this project, the investigation towards morphology and dielectric properties of single sample Strontium Titanate (ST) and Yttrium Iron Garnet (YIG), ST-YIG composite slabs (SYCS) and ST-YIG composites (SYC) were carried out. This is a pioneer work since no reports or studies were found on dielectric-magnetic slabs.

Each slab is made up of ST and YIG sample where for one slab, the samples were prepared via mechanical alloying (MA) method while the other were prepared via conventional solid state (SS) method. X-ray Diffraction (XRD) was employed for phase identification and purity of the samples. Since the ST-YIG composites prepared were multiphase, Rietveld refinement method was used to estimate the phase composition in each sample. MA method successfully reduced the sintering temperature for the reaction to occur at a much lower temperature compare to SS method. The surfaces of the sample were visualized using Field emission scanning electron microscopy (FESEM) and the average grain size was calculated. From FESEM images, MA method produced very fine particles in nano-scale while SS method in micro-scale.

The slabs were sintered at 1300°C with different sintering hours from 10 hours to 20 hours at intervals of 2 hours for SS method whereas for MA method, it was sintered at 1200°C. The samples for the slab were co-joined strongly through diffusional processes where no welding was involved. The junction properties were studied. FESEM images were also taken of the cross-sectional area of the slab and the diffusion of ST into YIG and vice versa can be observed at the junction. This only occurs for the slab prepared via SS method. The diffusion depth of both samples of the composite slab was determined via EDX. The distance at the junction where the ions moved from one compound to the other during the diffusion process is calculated. Movement of ions in the samples is dependent on the different sintering hours. However, for the slab

prepared via MA method, a slight diffusion occurs but the samples do not stick together. This is probably due to the continuous network of grain in YIG which only indicated the initial stage of sintering. The increased on migration of grain boundary increased the driving force for neck growth. Since surface diffusion and lattice diffusion dominated, therefore no interdiffusion process happened on the surface contact of ST and YIG. Thus, interstitial lattice diffusion among ST and YIG were difficult to obtain.

To understand the charge stored and energy dissipated, the dielectric properties of samples were investigated. Since the samples are multi-phase, hence the dielectric constant obtained is a contribution from different phases. Generally, the dielectric constant of the samples increases with the rise in temperature and decreases with frequency. The samples prepared via SS method have the best dielectric properties among the samples possibly due to the fine grain size of ST with large grain size of YIG produced denser grains by increasing the insulating grain boundary volume. For the slabs prepared via SS method, the dielectric constant and dielectric loss factor follows the trend of YIG rather than ST. The slabs produced better dielectric properties with higher value of dielectric constant and lower dielectric loss factor compared with single sample YIG. Therefore, it may be useful in microwave applications such as tunable HTS (high temperature superconducting) microwave filters. Analysis using complex modulus was also done on the samples to verify the polarization mechanism involved in the samples and slabs.

Abstrak tesis yang dikemukakan kepada Senat Universiti Putra Malaysia
sebagai memenuhi keperluan untuk ijazah Doktor Falsafah

**MIKROSTRUKTUR DAN SIFAT DIELEKTRIK BAGI SIMPANGAN
DWI-LAPISAN YTTRIUM IRON GARNET-STRONTIUM TITANATE DAN
SIMPANGAN KOMPOSIT**

Oleh

WONG SWEE YIN

Januari 2017

Pengerusi : Jumiah Hassan, PhD
Fakulti : Sains

Dalam projek ini, siasatan terhadap morfologi dan sifat dielektrik kepada Strontium Titanate dan Yttrium Iron Garnet sampel tunggal, papak komposit ST-YIG (SYCS) dan komposit ST-YIG (SYC) telah dijalankan. Ini adalah kerja perintis di mana tiada siasatan pernah dilakukan terhadap papak dielektrik-magnetik.

Setiap papak terdiri daripada ST dan YIG sampel di mana untuk satu papak, sampel telah disediakan melalui kaedah mekanikal pengalioian (MA) manakala yang lain telah disediakan melalui kaedah konvensional keadaan pepejal (SS). X-ray Diffraction (XRD) telah digunakan untuk mengenal pasti fasa dan ketulenan sampel. Oleh kerana sampel-sampel yang disediakan adalah berbilang fasa, maka kaedah penyempurnaan Rietveld telah digunakan untuk menganggarkan komposisi fasa dalam setiap sampel. Kaedah MA berjaya meningkatkan kereaktifan serbuk campuran dengan menurunkan suhu pensinteraan untuk tindak balas berlaku berbanding dengan kaedah SS.

Papak telah disinterkan pada 1300°C dengan masa pensinteran yang berbeza dari 10 jam hingga 20 jam pada selang 2 jam untuk kaedah SS manakala untuk kaedah MA, ia disinterkan pada 1200°C. Sampel papak telah bercantum dengan kuat melalui proses resapan di mana tiada kimpalan terlibat. Sifat simpangan telah dikaji. Imej FESEM juga diambil daripada kawasan keratan rentas papak dan peresapan ST ke YIG dan sebaliknya boleh diperhatikan di persimpangannya. Ini hanya berlaku bagi papak yang disediakan melalui kaedah SS. Kedalaman peresapan bagi kedua-dua sampel papak komposit telah ditentukan melalui EDX. Jarak di persimpangan di mana ion bergerak dari satu kawasan ke kawasan yang lain semasa proses peresapan dapat dikira. Pergerakan ion dalam sampel adalah bergantung kepada masa pensinteran yang berbeza. Walau bagaimanapun, bagi papak yang disediakan melalui kaedah MA, peresapan hanya berlaku sedikit tetapi sampel tidak bercantum bersama-sama. Ini mungkin disebabkan oleh rangkaian berterusan gandum YIG yang hanya menunjukkan peringkat

awal pensinteran. Peningkatan penghijrahan bagi sempadan bijian meningkatkan daya penggerak bagi pertumbuhan leher. Oleh sebab peresapan permukaan dan peresapan kekisi dikuasai, maka tiada proses peresapan dalaman berlaku pada sentuhan permukaan ST dan YIG. Oleh itu, peresapan kekisi pada celahan antara ST dan YIG sukar didapati.

Untuk memahami pengumpulan cas dan tenaga lesapan, sifat-sifat dielektrik sampel telah disiasat. Oleh sebab sampel mengandungi pelbagai fasa, maka pemalar dielektrik yang diperolehi adalah sumbangan daripada fasa yang berbeza. Secara umumnya, pemalar dielektrik sampel meningkat dengan kenaikan suhu dan berkurang dengan kekerapan. Sampel disediakan melalui kaedah SS mempunyai sifat dielektrik yang terbaik di kalangan sampel mungkin disebabkan oleh saiz butiran halus ST dengan saiz butiran besar YIG lalu menghasilkan bijirin padat dengan meningkatkan jumlah sempadan bijian penebat. Bagi papak yang disediakan melalui kaedah SS, pemalar dielektrik dan faktor kehilangan dielektrik mengikuti trend YIG bukannya ST. Papak yang dihasilkan mempunyai sifat dielektrik yang lebih baik dengan nilai yang lebih tinggi daripada pemalar dielektrik dan faktor kehilangan dielektrik yang lebih rendah berbanding dengan sampel YIG tunggal. Oleh itu, ia mungkin berguna dalam aplikasi gelombang mikro seperti HTS merdu (suhu tinggi superkonduktor) penapis gelombang mikro. Analisis terhadap modulus kompleks juga telah dijalankan ke atas sampel untuk mengesahkan mekanisme polarisasi yang terlibat dalam sampel dan papak.

ACKNOWLEDGEMENTS

First of all, I would like to express my deepest gratitude and appreciation to my supervisor, Assoc. Prof. Dr. Jumiah Hassan for giving me this opportunity to further my study on dielectric science by accomplishing this project. I am grateful to have Assoc. Prof. Dr. Jumiah Hassan as my supervisor for providing me excellent guidance and support.

Besides, I would like to acknowledge my late supervisory committee, the late Assoc. Prof. Dr. Mansor Hashim for giving me valuable advice, guidance and new knowledge throughout the completion of this project. I would also like to extend my sincere appreciation to my other supervisory committee, Assoc. Prof. Dr. Wan Mohammad Daud Wan Yusoff for his help and guidance.

Special thanks to my lab mates, Alex See, Tan Foo Khoon, Leow Chun Yan, and Wong Yick Jeng who had assisted me throughout my project and thesis writing. I would like to express my sincere appreciation to the staffs and technicians of Faculty of Science, ITMA and also the staffs at Hi-Tech Company for their equipment support throughout this project.

Finally, I wish to thank my parents, siblings and my lovely friends for their understanding and encouragement. Also, I would like to thank NSF scholarship for the 3-year financial support.

This thesis was submitted to the Senate of Universiti Putra Malaysia and has been accepted as fulfilment of the requirement for the degree of Doctor of Philosophy. The members of the Supervisory Committee were as follows:

Jumiah Hassan, PhD
Associate Professor
Faculty of Science
Universiti Putra Malaysia
(Chairman)

Mansor Hashim, PhD
Associate Professor
Faculty of Science
Universiti Putra Malaysia
(Member)

Wan Mohammad Daud Wan Yusoff, PhD
Associate Professor
Faculty of Science
Universiti Putra Malaysia
(Member)

ROBIAH BINTI YUNUS, PhD
Professor and Dean
School of Graduate Studies
Universiti Putra Malaysia

Date:

Declaration by graduate student

I hereby confirm that:

- this thesis is my original work;
- quotations, illustrations and citations have been duly referenced;
- this thesis has not been submitted previously or concurrently for any other degree at any other institutions;
- intellectual property from the thesis and copyright of thesis are fully-owned by Universiti Putra Malaysia, as according to the Universiti Putra Malaysia (Research) Rules 2012;
- written permission must be obtained from supervisor and the office of Deputy Vice-Chancellor (Research and Innovation) before thesis is published (in the form of written, printed or in electronic form) including books, journals, modules, proceedings, popular writings, seminar papers, manuscripts, posters, reports, lecture notes, learning modules or any other materials as stated in the Universiti Putra Malaysia (Research) Rules 2012;
- there is no plagiarism or data falsification/fabrication in the thesis, and scholarly integrity is upheld as according to the Universiti Putra Malaysia (Graduate Studies) Rules 2003 (Revision 2012-2013) and the Universiti Putra Malaysia (Research) Rules 2012. The thesis has undergone plagiarism detection software.

Signature: _____

Date: _____

Name and Matric No.: Wong Swee Yin (GS20578)

Declaration by Members of Supervisory Committee

This is to confirm that:

- the research conducted and the writing of this thesis was under our supervision;
- supervision responsibilities as stated in the Universiti Putra Malaysia (Graduate Studies) Rules 2003 (Revision 2012-2013) are adhered to.

Signature: _____
Name of
Chairman of
Supervisory
Committee: Assoc. Prof. Dr. Jumiah Hassan

Signature: _____
Name of
Member of
Supervisory
Committee: Assoc. Prof. Dr. Mansor Hashim

Signature: _____
Name of
Member of
Supervisory
Committee: Assoc. Prof. Dr. Wan Mohammad Daud Wan Yusoff

TABLE OF CONTENTS

		PAGE
ABSTRACT		i
ABSTRAK		iii
ACKNOWLEDGEMENTS		v
APPROVAL		vi
DECLARATION		viii
LIST OF TABLES		xii
LIST OF FIGURES		xiv
LIST OF SYMBOLS		xxii
LIST OF ABBREVIATIONS		xxiii
CHAPTER		
1	INTRODUCTION	1
	1.1 Background of Project	1
	1.2 Problem Statement	1
	1.3 Benefit of Research	2
	1.4 Conventional Solid State Method (SS)	2
	1.5 Mechanical Alloying Method (MA)	3
	1.6 Scope of Research	4
	1.7 Objectives	4
2	LITERATURE REVIEWS	5
	2.1 General	5
	2.2 Strontium Titanate (ST)	5
	2.3 Yttrium Iron Garnet (YIG)	6
	2.4 Solid State Sintering	7
	2.5 Theory of Dielectric	8
	2.6 Polarization	9
3	METHODOLOGY	12
	3.1 General	12
	3.2 Sample Preparation Using Conventional Solid State Method (SS)	13
	3.2.1 Flow Chart of Conventional Solid State Method	13
	3.2.2 Raw Materials	15
	3.2.3 Milling	15
	3.2.4 Pre-sintering	15
	3.2.5 Grinding and Sieving	16
	3.2.6 Moulding	16
	3.2.7 Sintering	16
	3.3 Sample Preparation Using Conventional Solid State Method (SS)	17
	3.3.1 Flow Chart of Mechanical Alloying Method	17
	3.3.2 Raw Materials	17
	3.3.3 Milling	18
	3.3.4 Moulding	18
	3.3.5 Sintering	19

3.4	Fabrication of ST-YIG Composite Slabs (SYCS)	19
3.5	Sample Preparation of ST-YIG Composites (SYC)	21
3.5.1	Raw Materials	21
3.5.2	Milling	22
3.5.3	Moulding	23
3.5.4	Sintering	23
3.6	Sample Characterization	23
3.6.1	Phase and Structural Analysis	23
3.6.2	Microstructural Analysis	23
3.6.3	Dielectric Measurement	24
4	RESULTS AND DISCUSSION	25
4.1	General	25
4.2	Conventional Solid State Method	26
4.2.1	Strontium Titanate (ST)	26
4.2.2	Yttrium Iron Garnet (YIG)	34
4.3	Mechanical Alloying Method	41
4.3.1	Strontium Titanate (ST)	41
4.3.2	Yttrium Ion Garnet (YIG)	45
4.4	Strontium Titanate-Yttrium Iron Garnet Composite Slab (SYCS)	49
4.4.1	Conventional Solid State Method (SS_SYCS)	49
4.4.2	Mechanical Alloying Method (MA_SYCS)	76
4.5	Strontium Titanate-Yttrium Iron Garnet Composite (SYC)	96
4.5.1	Conventional Solid State Method (SS_SYC)	96
4.5.2	Mechanical Alloying Method (MA_SYC)	117
5	CONCLUSION AND SUGGESTIONS	138
5.1	Conclusion	138
5.2	Suggestions	139
	BIBLIOGRAPHY	140
	APPENDICES	146
	BIODATA OF STUDENT	153
	LIST OF PUBLICATION	154

LIST OF TABLES

TABLE		PAGE
3.1	Starting materials for Strontium Titanate	15
3.2	Starting materials for Yttrium Iron Garnet	15
3.3	Strontium Titanate sintered at different sintering temperatures	16
3.4	Yttrium Iron Garnet sintered at different sintering temperatures	16
3.5	Series of ST-YIG composite slabs prepared by solid state method at different sintering hours	20
3.6	Series of ST-YIG composite slabs prepared by mechanical alloying method at different sintering hours	20
3.7	Series of Strontium Titanate and Yttrium Iron Garnet composites prepared by solid state method at different compositions	22
3.8	Series of Strontium Titanate and Yttrium Iron Garnet composites prepared by mechanical alloying method at different compositions	22
4.1	Average grain size of Strontium Titanate sintered at different sintering temperatures	29
4.2	Average grain size of Yttrium Iron Garnet sintered at different sintering temperatures	36
4.3	Average grain size of Strontium Titanate before and after sintering at 1000 °C	43
4.4	Average grain size of Yttrium Iron Garnet before and after sintering at 1200 °C	47
4.5	Average grain size for ST and YIG in SS_SYCS1 after sintering at 1300 °C for 10 hours	50
4.6	Average grain size for ST and YIG in SS_SYCS2 after sintering at 1300 °C for 12 hours	51
4.7	Average grain size for ST and YIG in SS_SYCS3 after sintering at 1300 °C for 14 hours	52

4.8	Average grain size for ST and YIG in SS_SYCS4 after sintering at 1300 °C for 16 hours	53
4.9	Average grain size for ST and YIG in SS_SYCS5 after sintering at 1300 °C for 18 hours	54
4.10	Average grain size for ST and YIG in SS_SYCS6 after sintering at 1300 °C for 20 hours	55
4.11	Diffusion depth for ST and YIG at the cross section of SS_SYCS samples	57
4.12	Average grain size for ST in MA_SYCS samples after sintering at 1200 °C for 10 hours, 12 hours, 14 hours, 16 hours, 18 hours and 20 hours	78
4.13	Expected Composition and Actual Composition for SS_SYC samples	97
4.14	Expected Composition and Actual Composition for MA_SYC samples	118

LIST OF FIGURES

FIGURE		PAGE
2.1	Atomic structure of Strontium Titanate	5
2.2	Mechanisms contribute to the sintering of crystalline particles	7
2.3	Capacitor made of two electrode plates	8
2.4	Typical responses of the total polarizability of a crystal as a function of electric field frequency	11
3.1	Flow chart for preparation of Strontium Titanate and Yttrium Iron Garnet at different sintering temperatures using conventional solid state method	14
3.2	Flow chart for preparation of Strontium Titanate and Yttrium Iron Garnet using mechanical alloying method	17
3.3	Vial and grinding balls	18
3.4	SPEX SamplePrep 8000D Mixer/Mill	18
3.5	Diagram of fabrication of ST-YIG composite slabs	19
3.6	Flow chart of sample preparation of ST-YIG composites using conventional solid state method and mechanical alloying method at different compositions	21
4.1	XRD patterns of Strontium Titanate at different sintering temperatures	27
4.2	Structure diagram of Strontium Titanate	27
4.3	FESEM micrographs and histograms of Strontium Titanate sintered at (a) 1100 °C, (b) 1200 °C and (c) 1300 °C	29
4.4	Relative permittivity of Strontium Titanate sintered at (a) 1100 °C, (b) 1200 °C and (c) 1300 °C with respect to frequency at selected temperatures	31
4.5	Dielectric loss factor of Strontium Titanate sintered at (a) 1100 °C, (b) 1200 °C and (c) 1300 °C with respect to frequency at selected temperatures	33
4.6	XRD patterns of Yttrium Iron Garnet at different sintering temperatures	34

4.7	Structure diagram of Yttrium Iron Garnet	35
4.8	FESEM micrographs and histograms of Yttrium Iron Garnet sintered at (a) 1300 °C, (b) 1350 °C and (c) 1400 °C	36
4.9	Relative permittivity of Yttrium Iron Garnet sintered at (a) 1300 °C, (b) 1350 °C and (c) 1400 °C with respect to frequency at selected temperatures	38
4.10	Dielectric loss factor of Yttrium Iron Garnet sintered at (a) 1300 °C, (b) 1350 °C and (c) 1400 °C with respect to frequency at selected temperatures	40
4.11	XRD patterns of Strontium Titanate	41
4.12	Structure diagram of Strontium Titanate	42
4.13	TEM micrograph and histogram of as-milled Strontium Titanate before sintering at 1000 °C	42
4.14	FESEM micrograph and histogram of Strontium Titanate after sintering at 1000 °C	43
4.15	Relative permittivity of Strontium Titanate sintered at 1000 °C with respect to frequency at selected temperatures	44
4.16	Dielectric loss factor of Strontium Titanate sintered at 1000 °C with respect to frequency at selected temperatures	45
4.17	XRD patterns of Yttrium Iron Garnet	46
4.18	Structure diagram of Yttrium Iron Garnet	46
4.19	TEM micrograph and histogram of as-milled Yttrium Iron Garnet before sintering at 1200 °C	47
4.20	FESEM micrograph and histogram of Yttrium Iron Garnet after sintering at 1200 °C	47
4.21	Relative permittivity of Yttrium Iron Garnet sintered at 1200 °C	48
4.22	Dielectric loss factor of Yttrium Iron Garnet sintered at 1200 °C	49
4.23	FESEM photographs and histogram of (a) ST, (b) YIG and (c) cross section of SS_SYCS1 after sintering at 1300 °C for 10 hours	50
4.24	FESEM photographs and histogram of (a) ST, (b) YIG and (c) cross section of SS_SYCS2 after sintering at 1300 °C for 12	51

	hours	
4.25	FESEM photographs and histogram of (a) ST, (b) YIG and (c) cross section of SS_SYCS3 after sintering at 1300 °C for 14 hours	52
4.26	FESEM photographs and histogram of (a) ST, (b) YIG and (c) cross section of SS_SYCS4 after sintering at 1300 °C for 16 hours	53
4.27	FESEM photographs and histogram of (a) ST, (b) YIG and (c) cross section of SS_SYCS5 after sintering at 1300 °C for 18 hours	54
4.28	FESEM photographs and histogram of (a) ST, (b) YIG and (c) cross section of SS_SYCS6 after sintering at 1300 °C for 20 hours	55
4.29	Average grain sizes for both ST and YIG in SS_SYCS samples, and ST (inset) sintered at 1300 °C at selected sintering times	56
4.30	Diffusion depth for ST and YIG at the cross section of SS_SYCS samples	57
4.31	Relative permittivity of SS_SYCS1 sintered at 1300 °C for 10 hours	59
4.32	Relative permittivity of SS_SYCS2 sintered at 1300 °C for 12 hours	59
4.33	Relative permittivity of SS_SYCS3 sintered at 1300 °C for 14 hours	60
4.34	Relative permittivity of SS_SYCS4 sintered at 1300 °C for 16 hours	60
4.35	Relative permittivity of SS_SYCS5 sintered at 1300 °C for 18 hours	61
4.36	Relative permittivity of SS_SYCS6 sintered at 1300 °C for 20 hours	61
4.37	Dielectric loss factor of SS_SYCS1 sintered at 1300 °C for 10 hours	62
4.38	Dielectric loss factor of SS_SYCS2 sintered at 1300 °C for 12 hours	63

4.39	Dielectric loss factor of SS_SYCS3 sintered at 1300 °C for 14 hours	63
4.40	Dielectric loss factor of SS_SYCS4 sintered at 1300 °C for 16 hours	64
4.41	Dielectric loss factor of SS_SYCS5 sintered at 1300 °C for 18 hours	64
4.42	Dielectric loss factor of SS_SYCS6 sintered at 1300 °C for 20 hours	65
4.43	Loss tangent of SS_SYCS1 sintered at 1300 °C for 10 hours	66
4.44	Loss tangent of SS_SYCS2 sintered at 1300 °C for 12 hours	66
4.45	Loss tangent of SS_SYCS3 sintered at 1300 °C for 14 hours	67
4.46	Loss tangent of SS_SYCS4 sintered at 1300 °C for 16 hours	67
4.47	Loss tangent of SS_SYCS5 sintered at 1300 °C for 18 hours	68
4.48	Loss tangent of SS_SYCS6 sintered at 1300 °C for 20 hours	68
4.49	Frequency dependence of (a) real part of modulus, (b) imaginary part of modulus of SS_SYCS1 sintered at 1300 °C for 10 hours	70
4.50	Frequency dependence of (a) real part of modulus, (b) imaginary part of modulus of SS_SYCS2 sintered at 1300 °C for 12 hours	71
4.51	Frequency dependence of (a) real part of modulus, (b) imaginary part of modulus of SS_SYCS3 sintered at 1300 °C for 14 hours	72
4.52	Frequency dependence of (a) real part of modulus, (b) imaginary part of modulus of SS_SYCS4 sintered at 1300 °C for 16 hours	73
4.53	Frequency dependence of (a) real part of modulus, (b) imaginary part of modulus of SS_SYCS5 sintered at 1300 °C for 18 hours	74
4.54	Frequency dependence of (a) real part of modulus, (b) imaginary part of modulus of SS_SYCS6 sintered at 1300 °C for 20 hours	75
4.55	FESEM photographs of (a)-(f) ST and (g)-(l) YIG of MA_SYCS samples after sintering at 1200 °C for 10 hours, 12	78

hours, 14 hours, 16 hours, 18 hours and 20 hours

4.56	Relative permittivity of MA_SYCS1 sintered at 1300 °C for 10 hours	80
4.57	Relative permittivity of MA_SYCS2 sintered at 1300 °C for 12 hours	80
4.58	Relative permittivity of MA_SYCS3 sintered at 1300 °C for 14 hours	81
4.59	Relative permittivity of MA_SYCS4 sintered at 1300 °C for 16 hours	81
4.60	Relative permittivity of MA_SYCS5 sintered at 1300 °C for 18 hours	82
4.61	Relative permittivity of MA_SYCS6 sintered at 1300 °C for 20 hours	82
4.62	Dielectric loss factor of MA_SYCS1 sintered at 1200 °C for 10 hours	83
4.63	Dielectric loss factor of MA_SYCS2 sintered at 1200 °C for 12 hours	84
4.64	Dielectric loss factor of MA_SYCS3 sintered at 1200 °C for 14 hours	84
4.65	Dielectric loss factor of MA_SYCS4 sintered at 1200 °C for 16 hours	85
4.66	Dielectric loss factor of MA_SYCS5 sintered at 1200 °C for 18 hours	85
4.67	Dielectric loss factor of MA_SYCS6 sintered at 1200 °C for 20 hours	86
4.68	Loss tangent of MA_SYCS1 sintered at 1200 °C for 10 hours	87
4.69	Loss tangent of MA_SYCS2 sintered at 1200 °C for 12 hours	87
4.70	Loss tangent of MA_SYCS3 sintered at 1200 °C for 14 hours	88
4.71	Loss tangent of MA_SYCS4 sintered at 1200 °C for 16 hours	88
4.72	Loss tangent of MA_SYCS5 sintered at 1200 °C for 18 hours	89
4.73	Loss tangent of MA_SYCS6 sintered at 1200 °C for 20 hours	89

4.74	Frequency dependence of (a) real part of modulus, (b) imaginary part of modulus of MA_SYCS1 sintered at 1200 °C for 10 hours	91
4.75	Frequency dependence of (a) real part of modulus, (b) imaginary part of modulus of MA_SYCS2 sintered at 1200 °C for 12 hours	92
4.76	Frequency dependence of (a) real part of modulus, (b) imaginary part of modulus of MA_SYCS3 sintered at 1200 °C for 14 hours	93
4.77	Frequency dependence of (a) real part of modulus, (b) imaginary part of modulus of MA_SYCS4 sintered at 1200 °C for 16 hours	94
4.78	Frequency dependence of (a) real part of modulus, (b) imaginary part of modulus of MA_SYCS5 sintered at 1200 °C for 18 hours	95
4.79	Frequency dependence of (a) real part of modulus, (b) imaginary part of modulus of MA_SYCS6 sintered at 1200 °C for 20 hours	96
4.80	XRD patterns of SS_SYC samples at different compositions	97
4.81	FESEM photographs of (a) SS_SYC1, (b) SS_SYC2, (c) SS_SYC3, (d) SS_SYC4, (e) SS_SYC5 and (f) SS_SYC6 after sintering at 1300 °C	99
4.82	Relative permittivity of (a) SS_SYC1, (b) SS_SYC2, (c) SS_SYC3, (d) SS_SYC4, (e) SS_SYC5 and (f) SS_SYC6 sintered at 1300 °C for 10 hours	103
4.83	Dielectric loss factor of (a) SS_SYC1, (b) SS_SYC2, (c) SS_SYC3, (d) SS_SYC4, (e) SS_SYC5 and (f) SS_SYC6 sintered at 1300 °C for 10 hours	106
4.84	Loss tangent of (a) SS_SYC1, (b) SS_SYC2, (c) SS_SYC3, (d) SS_SYC4, (e) SS_SYC5 and (f) SS_SYC6 sintered at 1300 °C for 10 hours	110
4.85	Frequency dependence of (a) real part of modulus, (b) imaginary part of modulus of SS_SYC1 sintered at 1300 °C for 10 hours	111
4.86	Frequency dependence of (a) real part of modulus, (b) imaginary part of modulus of SS_SYC2 sintered at 1300 °C for	112

	10 hours	
4.87	Frequency dependence of (a) real part of modulus, (b) imaginary part of modulus of SS_SYC3 sintered at 1300 °C for 10 hours	113
4.88	Frequency dependence of (a) real part of modulus, (b) imaginary part of modulus of SS_SYC4 sintered at 1300 °C for 10 hours	114
4.89	Frequency dependence of (a) real part of modulus, (b) imaginary part of modulus of SS_SYC5 sintered at 1300 °C for 10 hours	115
4.90	Frequency dependence of (a) real part of modulus, (b) imaginary part of modulus of SS_SYC6 sintered at 1300 °C for 10 hours	116
4.91	XRD patterns of MA_SYC samples at different compositions	117
4.92	FESEM photographs of (a) MA_SYC1, (b) MA_SYC2, (c) MA_SYC3, (d) MA_SYC4, (e) MA_SYC5 and (f) MA_SYC6 after sintering at 1200 °C	119
4.93	Relative permittivity of (a) MA_SYC1, (b) MA_SYC2, (c) MA_SYC3, (d) MA_SYC4, (e) MA_SYC5 and (f) MA_SYC6 sintered at 1200 °C for 10 hours	123
4.94	Dielectric loss factor of (a) MA_SYC1, (b) MA_SYC2, (c) MA_SYC3, (d) MA_SYC4, (e) MA_SYC5 and (f) MA_SYC6 sintered at 1200 °C for 10 hours	127
4.95	Loss tangent of (a) MA_SYC1, (b) MA_SYC2, (c) MA_SYC3, (d) MA_SYC4, (e) MA_SYC5 and (f) MA_SYC6 sintered at 1200 °C for 10 hours	130
4.96	Frequency dependence of (a) real part of modulus, (b) imaginary part of modulus of MA_SYC1 sintered at 1200 °C for 10 hours	132
4.97	Frequency dependence of (a) real part of modulus, (b) imaginary part of modulus of MA_SYC2 sintered at 1200 °C for 10 hours	133
4.98	Frequency dependence of (a) real part of modulus, (b) imaginary part of modulus of MA_SYC3 sintered at 1200 °C for 10 hours	134
4.99	Frequency dependence of (a) real part of modulus, (b) imaginary part of modulus of MA_SYC4 sintered at 1200 °C	135

	for 10 hours	
4.100	Frequency dependence of (a) real part of modulus, (b) imaginary part of modulus of MA_SYC5 sintered at 1200 °C for 10 hours	136
4.101	Frequency dependence of (a) real part of modulus, (b) imaginary part of modulus of MA_SYC6 sintered at 1200 °C for 10 hours	137



LIST OF SYMBOLS

C	Capacitance
E	Electric field
Q	Magnitude of total charge
V	Potential difference
A	Area of each plate or cross-sectional area
d	Separation between the plates
C_o	Capacitance of parallel plates in vacuum
ϵ_0	Permittivity of free space
ϵ^*	Complex permittivity
ϵ	Permittivity of material
ϵ'_r	Relative permittivity
ϵ''_r	Relative dielectric loss factor
D	Displacement vector
P	Polarization

LIST OF ABBREVIATIONS

SS	Conventional solid state
MA	Mechanical alloying
ST	Strontium Titanate
YIG	Yttrium Iron Garnet
XRD	X-ray diffraction
FESEM	Field Emission Scanning Electron Microscope
EDX	Energy Dispersive X-ray Spectroscopy
ICSD	Inorganic Crystal Structure Database



CHAPTER 1

INTRODUCTION

1.1 Background of Project

In this project, a new development of diffusional change and the dielectric behavior of dielectric-magnetic composite slabs were studied. The samples were prepared using different preparation methods, conventional solid state method and mechanical alloying method.

Each preparation method produced a series of samples with different sintering hours, 10 hours - 20 hours at 2 hours intervals. The samples were Strontium Titanate (ST) and Yttrium Iron Garnet (YIG). ST was sintered at 1200 °C and 1000 °C respectively while YIG was sintered at 1400 °C and 1200 °C respectively for conventional solid state method and mechanical alloying method. Both samples were sandwiched together and sintered at a specific sintering temperature, 1300 °C and 1200 °C respectively with different sintering hours.

The purification and crystallinity of the samples were characterized using X-ray Diffraction (XRD), while the surface morphology and the diffusion depths were characterized using Field Emission Scanning Electron Microscope (FESEM) and Energy Dispersive X-ray Spectroscopy (EDX). The dielectric behavior of the samples was measured using Agilent High Resolution Analyzer at frequency ranges, 10 mHz - 1 MHz and Agilent 4294A Precision Impedance Analyzer at frequency ranges, 40 Hz - 10 MHz at different measuring temperatures, 30°C, 50°C - 250°C at 25°C intervals.

1.2 Problem Statement

In the past researches, there were some investigations and reports made on the diffusional and dielectric properties at the junction of the dielectric-dielectric composites slab. However, studies on the dielectric-magnetic composite slab have not been reported.

Diffusion process which occurred in solid state materials were studied especially for samples prepared using the sputtering technique, but diffusion process for samples prepared by conventional solid state method has not been investigated.

Dielectric behavior is usually studied in insulating materials, such as ceramics, glass, and etc. Based on past researches, ceramics which have high dielectric constant will also have high dielectric loss factor at high frequency range. Materials which exhibit high dielectric constant and low dielectric loss factor at high frequency range have not been developed.

1.3 Benefit of Research

In this project, there are some new findings which have not been discovered in previous works. Dielectric-magnetic composite slab is a new composite which may produce both dielectric and magnetic behavior at the same time. These new composite slabs were prepared by conventional solid state method and mechanical alloying method.

Grain growth and diffusion process for both dielectric and magnetic composite slab were analyzed at the junction of the composite slab. The dielectric behavior of the single sample and composite slab were analyzed and comparison between their properties was made. The morphological and diffusional changes and the dielectric behavior within the dielectric-magnetic bi-plate junctions were determined.

In addition, the dielectric-magnetic composite slabs are useful especially in electronic industry. It can be used as power insulation and charge storage in industry. Besides, it can also be used in microwave applications such as tunable HTS (high temperature superconducting) microwave filters.

1.4 Conventional Solid State Method (SS)

Conventional solid state method (SS) is a traditional method where two or more different starting materials will react together after heating to form the required products. This method which involves of mixing different powders is common to use to prepare a wide range of ceramic products, such as metal oxides, titanates, ferrites, silicates, and etc (Rahaman, 2003).

Conventional solid state method is a method which is widely used in preparation of polycrystalline ceramics. This method implicates the consolidation of fine powders to form a green body which is then sintered to produce a dense product with heterogeneous microstructure. These can be prepared by pressing it in pellet form. Solid state reaction relies on several parameters, such as size and shape of the particles, uniformity of the mixing, sintering temperature and time, and etc (Rahaman, 2003).

Solid state sintering resulted in atomic diffusion which leads to densification of the grains or coarsening of the microstructure. Changes in density, grain size, and pore size show the behavior on densification of grains. Coarsening process also undergoes the same changes as densification except pore size. Pores shrink during densification, while pores grow during coarsening. Moreover, surface diffusion, volume diffusion, grain boundary diffusion, viscous flow, plastic flow, and vapor transport from solid surfaces also contribute to the sintering process (Rahaman, 2003).

There are advantages and disadvantages using this method. This method can be used to prepare a large amount of the required products. High purification on the starting materials is not required and the cost of production is low (C. Barry Carter, M. Grant Norton, 2007). However, contamination of powder with impurities may happen during

the grinding process. Besides, particle size of powders is hard to control. This may produce chemically inhomogeneous product with complex microstructures. (Rahaman, 2003). Furthermore, high sintering temperature (above 1000 °C) is required for the materials to undergo chemical reaction among the reactants to produce the product.

1.5 Mechanical Alloying Method (MA)

Mechanical alloying method (MA) is a method which is similar to the conventional solid state method excluding the preparation of a green body. Mechanical alloying is a technique where two or more different compounds are mixed and milled together in a small high-speed shaker in dry condition. The mixture which forms solid solution, intermetallic, or amorphous phase after milling is a homogeneous alloy. These means material transfer is involved in this method (Suryanarayana, 2004).

Besides, this method induces chemical reactions during the milling process, such as mechanochemical reactions. This method can be used to prepare a variety of powders, such as oxides, carbides, nitrides, borides, and silicides (Rahaman, 2003). The important physical parameters required in this method are the raw materials, the mill, and the process variables. Raw materials normally have particle size in the range of 1-200 µm, which should be smaller than the size of the grinding ball. This method is carried out using SPEX SamplePrep 8000D Mixer/Mill, which is able to contain 8-20 g of the powder at a time depending on the size of the vials. The vials are clamped and swung energetically back and forth for several thousand times a minute. The grinding balls which are put together with the powder will collide with the powder and the vials. This technique is considered as high-energy milling due to the high velocities of grinding balls and the high speed of clamp motion.

There are three possibilities based on the mechanism of mechanochemical reaction. The first possibility may be due to the solid state diffusion mechanism. During the milling process, a slightly increase in temperature in the mill lower the activation energy of the mixtures and therefore leads to diffusion process. Since heating of the mill occurs, the sintering temperature for the mixtures is obviously lower than that as compared to solid state method. The second possibility may be due to the local melting during the milling process where exothermic reaction occurs and releases heat to the surrounding. The third possibility may cause by a form of self-propagating process at high temperature. In highly exothermic reaction, the heat that released sustains the reaction.

The advantage of using this method is simple preparation method especially for silicides and carbides which have a narrow compositional range which are hardly to produce and need to sinter at high temperatures. Besides, this method can produce alloy at low temperature without melting them. This method is able to reduce the particle size in large dimension to nanometer. Conversely, contamination may occur due to the integration of impurities from the mill and milling medium into the powders. Besides, the temperature change in the mill during the milling process is hard to control (Rahaman, 2003).

1.6 Scope of Research

Strontium Titanate is one of the famous ferroelectric materials which exhibit large dielectric constant for sintered ceramics while Yttrium Iron Garnet is a kind of soft ferromagnetic materials which exhibit high Q factor in microwave applications. The dielectric-magnetic composite slabs (Strontium Titanate-Yttrium Iron Garnets composite slabs) and dielectric-magnetic composite (Strontium Titanate-Yttrium Iron Garnets composite) were prepared by conventional solid state method and mechanical alloying method. Each composite slabs and composites were sintered at 1300 °C and 1200 °C for 10 hours respectively. The dielectric properties of the samples were measured using Agilent High Resolution Analyzer at frequency range of 10 mHz to 1 MHz and Agilent 4294A Precision Impedance Analyzer at frequency range of 40 Hz to 10 MHz at 30°C, 50°C - 250°C at 25°C intervals. The morphological and diffusional changes and the dielectric behavior within the dielectric-magnetic bi-plate junctions offer the advancement of new knowledge in this multilayer composite.

1.7 Objectives

The objectives of the present study were developed as follows:

1. To prepare Strontium Titanate (ST), Yttrium Iron Garnet (YIG), Strontium Titanate-Yttrium Iron Garnets composites slab (SYCS), and Strontium Titanate-Yttrium Iron Garnets composites (SYC) via conventional solid state method and mechanical alloying method and characterize their crystallinity, surface morphology and diffusional properties of the bi-plate junctions via XRD, FESEM including EDX and other morphological study techniques.
2. To characterize the dielectric behavior for single samples, composite slabs and composites at different measuring temperatures.
3. To understand and explain the effects of morphological and diffusional changes and the dielectric behavior of the junctions in the composite slabs.

Therefore, the present study required to respond to the following research questions:

1. Would ST, YIG, SYCS, and SYC successfully prepared via conventional solid state method and mechanical alloying method?
2. Would XRD, FESEM including EDX and other morphological study techniques analyze the samples' crystallinity, surface morphology and diffusional properties of the bi-plate junctions?
3. Would the dielectric behavior for single samples, composite slabs and composites been analyzed at different measuring temperatures?
4. Would the effects of morphological and diffusional changes and the dielectric behavior of the junctions in the composite slabs been explained?

BIBLIOGRAPHY

- Ahmed R., Moslehuddin A., Mahmood Z. H. and Akther Hossain A. (2015). Weak ferromagnetism and temperature dependent dielectric properties of Zn_{0.9}Ni_{0.1}O diluted magnetic semiconductor. *Materials Research Bulletin*, 63, 32-40.
- Bajpai, P. and Singh, K. (2011). Dielectric relaxation and ac conductivity study of Ba(Sr_{1/3}Nb_{2/3})O₃. *Physica B*, 406, 1226-1232.
- Barry, C. C., Norton, M. G. (2007). *Ceramic Materials Science and Engineering*. New York: Springer.
- Bunget, I. and Popescu, M. (1984). *Physics of Solid Dielectrics*. New York: Elsevier.
- Burn, I., Neirman, S. (1982). Dielectric properties of donor-doped polycrystalline SrTiO₃. *Journal of Materials Science*, 17, 3510-3524.
- Castro-Rodriguez, R., Palomares-Sanchez, S., Watts, B. E., & Leccabue, F. (2003). A simple model to study the perovskite phase formation of SrTiO₃ deposited by pulsed laser ablation. *Materials Letters*, 57, 3958-3963. [http://doi.org/10.1016/S0167-577X\(03\)00247-7](http://doi.org/10.1016/S0167-577X(03)00247-7)
- Chen, D., Jiao, X., & Zhang, M. (2000). Hydrothermal synthesis of strontium titanate powders with nanometer size derived from different precursors. *Journal of the European Ceramic Society*, 20(9), 1261-1265. [http://doi.org/10.1016/S0955-2219\(00\)00003-0](http://doi.org/10.1016/S0955-2219(00)00003-0)
- Chen, H., Zhong, Y., Hu, W., Gottstein, G. (2007). A diffusion bonding model for the consolidation process of matrix-coated fiber-reinforced composites. *Materials Science and Engineering A*, 452-453, 625-632. <http://doi.org/10.1016/j.msea.2006.10.104>
- Chen, L., Ong, C., Neo, C., and Varadan, V. (2004). *Microwave Electronics, measurement and material characterisation*. West Sussex: John Wiley & Sons Ltd.
- Chen, L., Zhang, S., Wang, L., Xue, D., & Yin, S. (2009). Preparation and photocatalytic properties of strontium titanate powders via sol-gel process. *Journal of Crystal Growth*, 311(3), 746-748. <http://doi.org/10.1016/j.jcrysgro.2008.09.185>
- Choudhury, P. R., & Krupanidhi, S. B. (2007). Studies on strontium titanate/barium zirconate superlattices. *Solid State Communications*, 143(4-5), 223-227. <http://doi.org/10.1016/j.ssc.2007.05.017>
- Cui, H., Zayat, M., & Levy, D. (2007). Controlled homogeneity of the precursor gel in the synthesis of SrTiO₃ nanoparticles by an epoxide assisted sol-gel route. *Journal of Non-Crystalline Solids*, 353(11-12), 1011-1016. <http://doi.org/10.1016/j.jnoncrysol.2007.01.009>

- Da Silva, L. F., Maia, L. J. Q., Bernardi, M. I. B., Andr s, J. A., & Mastelaro, V. R. (2011). An improved method for preparation of SrTiO₃ nanoparticles. *Materials Chemistry and Physics*, 125(1–2), 168–173. <http://doi.org/10.1016/j.matchemphys.2010.09.001>
- Fleury, P. A., Scott, J. F., & Worlock, J. M. (1968). Soft Phonon Modes and the 110 K Phase Transition in SrTiO₃. *Physical Review Letters*, 21(1), 16–19. <http://doi.org/10.1103/PhysRevLett.21.16>
- George, C. N., Thomas, J. K., Jose, R., Kumar, H. P., Suresh, M. K., Kumar, V. R., Shobana, W. P. R., Koshy, J. (2009). Synthesis and characterization of nanocrystalline strontium titanate through a modified combustion method and its sintering and dielectric properties. *Journal of Alloys and Compounds*, 486(1–2), 711–715. <http://doi.org/10.1016/j.jallcom.2009.07.045>
- Gerhardt R. (1994). Impedance and dielectric spectroscopy revisited: Distinguishing localized relaxation from long-range conductivity. *Journal of Physics Chemistry Solids*, 55, 1491-1506.
- Grosseau, P., Bachiorelli, A., Guilhot, B. (1997). Preparation of polycrystalline yttrium iron garnet ceramics. *Powder Technology*, 93, 247-251. [http://doi.org/10.1016/S0032-5910\(97\)03279-8](http://doi.org/10.1016/S0032-5910(97)03279-8)
- Herbert, J. M. (1992). *Ceramic Dielectrics and Capacitors*. UK: Gordon and Breach Science Publishers.
- Hodge, I., Ingram, M. and West, A. (1976). Impedance and modulus spectroscopy of polycrystalline solid electrolytes. *Journal of Electroanal Chemistry*, 74, 125-143.
- Hsing-I H., Chi-Shiung H., Chi-Yao T. and Li-Then M. (2015). Cobalt-substitution effect on dielectric properties of CuZn ferrites. *Ceramics International*, 41, 4140-4144.
- Ishikawa, H., Oohira, K., Nakajima, T., & Akiyama, T. (2008). Combustion synthesis of SrTiO₃ using different raw materials. *Journal of Alloys and Compounds*, 454(1–2), 384–388. <http://doi.org/10.1016/j.jallcom.2006.12.113>
- Jacob, K. T., Rajitha, G. (2012). Nonstoichiometry, defects and thermodynamic properties of YFeO₃, YFe₂O₄ and Y₃Fe₅O₁₂. *Solid State Ionics*, 224, 32-40.
- Jianjun, L., Chun-Gang D., Wei-Guo Y., Mei, W., Smith, R. and Hardy, J. (2003). Dielectric permittivity and electric modulus in Bi₂Ti₄O₁₁. *Journal of Chemical Physics*, 119, 2812-2819.
- Johnson, S. D., Glaser, E. R., Cheng, S., Hite, J. (2016). Dense nanocrystalline yttrium iron garnet films formed at room temperature by aerosol deposition. *Materials Research Bulletin*, 76, 365-369.

- Kang, S.-J. L. (2005). Sintering Processes. *Sintering*, 3–8. <http://doi.org/10.1016/B978-075066385-4/50001-7>
- Kang, S.-J. L. (2005). *Sintering: Densification, Grain Growth and Microstructure*. Oxford: Elsevier.
- Kim, M., Hong, S., Shin, N., Lee, H. Y., Shin, Y. (2016). Synthesis of strontium titanate nanoparticles using supercritical water. *Ceramics International*, 42, 17853-17857. <http://doi.org/10.1016/j.ceramint.2016.08.120>
- Klaytae, T., Panthong, P., & Thountom, S. (2013). Preparation of nanocrystalline strontium titanate (SrTiO₃) powder by sol-gel combustion method. *Scientific Research and Essays*, 8(1), 32–38. <http://doi.org/10.5897/SRE12.592>
- Lemke, F., Rheinheimer, W., Hoffmann, M. J. (2017). A comparison of power controlled flash sintering and conventional sintering of strontium titanate. *Scripta Materialia*, 130, 187-190. <http://doi.org/10.1016/j.scriptamat.2016.12.008>
- Li, L., Zhao, J., Gui, Z. (2004). The thermal sensitivity and dielectric properties of SrTiO₃ - based ceramics. *Ceramics International*, 30, 1073-1078. <http://doi.org/10.1016/j.ceramint.2003.12.027>
- Lyle, F. W. (1964). X-Ray Diffractometry of Low-Temperature Phase Transformations in Strontium Titanate. *Journal of Applied Physics*, 35(7), 2212. <http://doi.org/10.1063/1.1702820>
- Makarova, M., Dejneka, A., Franc, J., Drahokoupil, J., Jastrabik, L., & Trepakov, V. (2010). Soft chemistry preparation methods and properties of strontium titanate nanoparticles. *Optical Materials*, 32(8), 803–806. <http://doi.org/10.1016/j.optmat.2010.01.007>
- Migahed, M. D., Ishra, M., Fahmy, T., Barakat, A. (2004). Electric modulus and AC conductivity studies in conducting PPy composite films at low temperature. *Journal of Physics and Chemistry of Solids*, 65, 1121-1125. <http://doi.org/10.1016/j.jpcs.2003.11.039>
- Molak, A., Paluch, M., Pawlus, S., Klimontko, J., Ujma, Z., Gruszka, I. (2005). Electric modulus approach to the analysis of electric relaxation in highly conducting (Na_{0.75} Bi_{0.25})(Mn_{0.25} Nb_{0.75})O₃ ceramics. *Journal of Physics D: Applied Physics*, 38, 1450-1460. <http://doi.org/10.1088/0022-3727/38/9/019>
- Müller, K. A., & Burkard, H. (1979). SrTiO₃ : An intrinsic quantum paraelectric below 4 K. *Physical Review B*, 19(7), 3593–3602. <http://doi.org/10.1103/PhysRevB.19.3593>
- Nava, R., Callarotti, R., Ceva, H., & Martinet, A. (1968). Anomalous hypersonic attenuation in strontium titanate. *Physics Letters A*, 28(6), 456–457. [http://doi.org/10.1016/0375-9601\(68\)90494-5](http://doi.org/10.1016/0375-9601(68)90494-5)

- Neagu, A. M., Ciuchi, I. V., Curecheriu, P. and Mitoseriu, L. (2010). Impedance spectroscopy characterization of collagen samples. *Journal of Advanced Research in Physics*, 1, 1-4.
- Orhan, N., Aksoy, M., Eroglu, M. (1999). A new model for diffusion bonding and its application to duplex alloys. *Materials Science and Engineering A*, 271, 458-468. [http://doi.org/10.1016/S0921-5093\(99\)00315-9](http://doi.org/10.1016/S0921-5093(99)00315-9)
- Paiva, D. V. M., Silva, M. A. S., Ribeiro, T. S., Vasconcelos, I. F., Sombra, A. S. B., Góes, J. C., Fechine, P. B. A. (2015). Novel magnetic – dielectric composite ceramic obtained from $Y_3Fe_5O_{12}$ and $CaTiO_3$. *Journal of Alloys and Compounds*, 644, 763-769.
- Pal, M., & Chakravorty, D. (2000). Synthesis of nanocrystalline yttrium iron garnet by sol – gel route. *Physica E*, 5, 200–203. [http://doi.org/10.1016/S1386-9477\(99\)00040-5](http://doi.org/10.1016/S1386-9477(99)00040-5)
- Patra, B. S., Otta, S., & Bhattamisra, S. D. (2006). A kinetic and mechanistic study of thermal decomposition of strontium titanyl oxalate. *Thermochimica Acta*, 441(1), 84–88. <http://doi.org/10.1016/j.tca.2005.11.030>
- Petzelt, J., Gregora, I., Rychetský, I., Ostapchuk, T., Kamba, S., Vaněk, P., Waser, R. (2001). Polar grain boundaries in undoped $SrTiO_3$ ceramics. *Journal of the European Ceramic Society*, 21(15), 2681–2686. [http://doi.org/10.1016/S0955-2219\(01\)00345-4](http://doi.org/10.1016/S0955-2219(01)00345-4)
- Popovic, D., Romcevic, N., Spasovic, S., Dojcilovic, J., Golubovic, A., Nikolic, S. (2006). Dielectric, spectral and Raman scattering studies of Nd-doped $SrTiO_3$ single crystal. *Journal of Alloys and Compounds*.
- Poth, J., & Haberkorn, R. (2000). Combustion-synthesis of $SrTiO_3$ Part II. Sintering behaviour and surface characterization. *Journal of the European Ceramic Society*, 20, 715–723. [http://doi.org/http://dx.doi.org/10.1016/S0955-2219\(99\)00190-9](http://doi.org/http://dx.doi.org/10.1016/S0955-2219(99)00190-9)
- Qinghui Yang, H. Z. (2008). The magnetic and dielectric properties of microwave sintered yttrium iron garnet (YIG). *Materials Letters* 62, 2647-2650.
- Rahaman, M. N. (2003). *Ceramic Processing And Sintering*. USA: CRC Press.
- Raju, G. G. (2003). *Dielectrics in Electric Fields*. USA: Marcel Dekker, Inc.
- Ranjith Kumar E. and Jayaprakash R. (2014). The role of fuel concentration on particle size and dielectric properties of manganese substituted zinc ferrite nanoparticles. *Journal of Magnetism and Magnetic Materials*, 366, 33-39.
- Rao, V. L., Shekharam, T., Kumar, T. and Nagabhushanam, M. (2015). Effect of copper on impedance and dielectric studies of $Cu_xZn_{1-x}S$ mixed semiconductor compounds. *Material Chemistry and Physics*, 159, 83-92.

- Rheinheimer, W., B äurer, M., Chien, H., Rohrer, G. S., Handwerker, C. A., Blendell, J. E., Hoffmann, M. J. (2015). The equilibrium crystal shape of strontium titanate and its relationship to the grain boundary plane distribution. *Acta Materialia*, 82, 32-40.
- Rheinheimer, W., B äurer, M., Hoffmann, M. J. (2015). A reversible wetting transition in strontium titanate and its influence on grain growth and the grain boundary mobility. *Acta Materialia*, 101, 80-89.
- Ropp, R. C. (2003). *Solid State Chemistry*. USA: Elsevier.
- Satyanarayana, N. (2010). *Synthesis, characterization and transport studies of lithium based superionic conductors for solid state battery applications*, PhD Thesis, Pondicherry University, India.
- Shirzadi, A. A., Assadi, H., Wallach, E. R. (2001). Interface evolution and bond strength when diffusion bonding materials with stable oxide films. *Surface and Interface Analysis*, 31, 609-618.
- Solyman, L. and Walsh, D. (1979). *Lectures on the electrical properties of materials*, Great Britain: Oxford University Press.
- Song, T. K., Kim, J., Kwun, S. I., Kim, C. J., & Kim, J. J. (1996). Raman spectroscopy of quantum paraelectric SrTiO₃ fine particles. *Physica B: Condensed Matter*, 219–220(1–4), 538–540. [http://doi.org/10.1016/0921-4526\(96\)80482-0](http://doi.org/10.1016/0921-4526(96)80482-0)
- Suryanarayana, C. (2004). *Mechanical Alloying and Milling*. USA: Marcel Dekker.
- Tkach, A., Vilarinho, P. M., Senos, A. M. R., & Kholkin, A. L. (2005). Effect of nonstoichiometry on the microstructure and dielectric properties of strontium titanate ceramics. *Journal of the European Ceramic Society*, 25(12 SPEC. ISS.), 2769–2772. <http://doi.org/10.1016/j.jeurceramsoc.2005.03.137>
- Um, M. H., & Kumazawa, H. (2000). Hydrothermal synthesis of ferroelectric barium and strontium titanate extremely fine particles. *Journal of Materials Science*, 35(5), 1295–1300. <http://doi.org/10.1023/A:1004713226000>
- Wan F. F., W. A., Othman, M., Ain, M. F., Abdullah, N. S., Ahmad, Z. A. (2013). Studies on the formation of yttrium iron garnet (YIG) through stoichiometry modification prepared by conventional solid-state method. *Journal of the European Ceramic Society*, 33, 1317-1324.
- Wang, J., Yin, S., Zhang, Q., Saito, F., & Sato, T. (2003). Mechanochemical synthesis of SrTiO_{3-x}F_x with high visible light photocatalytic activities for nitrogen monoxide destruction. *J. Mater. Chem.*, 13(9), 2348–2352. <http://doi.org/10.1039/B303420H>
- Widodo, R. D., Manaf, A., Viktor, R. R. V., & Al-Janan, D. H. (2015). The Effect of Milling Times and Annealing on Synthesis of Strontium Titanate Ceramic s. *International Journal of Innovative Research in Advanced Engineering*, 2(12),

- Wong, S. Y., Hassan, J., & Hashim, M. (2009). Dielectric Properties of Strontium Titanate in the 1 MHz to 1.5 GHz Frequency Regions. *Solid State Science and Technology*, 17(1), 57–62. Retrieved from ISSN 0128-7389
- Wong, Y. J., Hassan, J., Hashim, M., Wong, S. Y., Leow, C. Y. (2011). Effect of Milling Time on Microstructure, Crystallite Size and Dielectric Properties of SrTiO₃ Ceramic Synthesized via Mechanical Alloying Method. *Advanced Materials Research*, 364, 388-392.
<http://doi.org/10.4028/www.scientific.net/AMR.364.388>
- Xian, T., Yang, H., Dai, J. F., Wei, Z. Q., Ma, J. Y., & Feng, W. J. (2011). Photocatalytic properties of SrTiO₃ nanoparticles prepared by a polyacrylamide gel route. *Materials Letters*, 65(21–22), 3254–3257.
<http://doi.org/10.1016/j.matlet.2011.07.019>
- Yan, L. C., Hassan, J., Hashim, M., Yin, W. S., Khoon, T. F., & Jeng, W. Y. (2011). Effect of Sintering Temperatures on the Microstructure and Dielectric Properties of SrTiO₃ Institute of Advanced Technology , Universiti Putra Malaysia , Malaysia. *World Applied Sciences Journal*, 14(7), 1091–1094.
- Yang, Q., Zhang, H., Liu, Y., Wen, Q., & Jia, L. (2008). The magnetic and dielectric properties of microwave sintered yttrium iron garnet (YIG). *Materials Letters*, 62(17–18), 2647–2650. <http://doi.org/10.1016/j.matlet.2008.01.040>
- Yaru, W., Yongping, P. and Panpan, Z. (2015). Investigation of dielectric relaxation in BaTiO₃ ceramics modified with BiYO₃ by impedance spectroscopy. *Journal of alloy and compounds*, 653, 596-603.
- Zhang, N., Li, Q., Huang, S., Yu, Y., Zheng, J., Cheng, C. and Wang, C. (2015). Dielectric relaxation in multiferroic La₂Ti₂O₇ ceramic. *Journal of alloys and compounds*, 652, 1-8.
- Zhang, S., Liu, J., Han, Y., Chen, B., & Li, X. (2004). Formation mechanisms of SrTiO₃ nanoparticles under hydrothermal conditions. *Materials Science and Engineering B: Solid-State Materials for Advanced Technology*, 110(1), 11–17. <http://doi.org/10.1016/j.mseb.2004.01.017>
- Zheludev, I. S. (1971). *Physics of Crystalline Dielectrics* . New York: Plenum Press.